

Diffusion of an annular plasma in positron acceleration

Francis F. Chen^{a)}

Electrical Engineering Department, University of California, Los Angeles, California 90095-1594, USA

(Received 7 August 2007; accepted 19 November 2007; published online 20 December 2007)

Electron acceleration to multi-GeV energies has been demonstrated using plasma wakefields in a tunnel-ionized plasma. However, coherent wakefields for positron acceleration may require hollow plasmas pre-ionized by a laser beam. The lifetime of such a plasma is determined by an unusual diffusion problem in which the diffusion rate varies by an order of magnitude inside the hole. The problem is solved by numerical differentiation without using a particle-in-cell code. The densities assumed in this work match those in existing positron experiments and are low compared with those in electron experiments. Future positron experiments at higher densities will not exhibit the nonlinear diffusion treated here because they will be dominated by recombination and tunneling ionization by the beam. © 2007 American Institute of Physics. [DOI: 10.1063/1.2824995]

I. INTRODUCTION

Energy doubling of the 42-GeV Stanford Linear Accelerator electron beam has been demonstrated by Blumenfeld *et al.*¹ using the wakefield acceleration mechanism.² The plasma is created by tunnel ionization³⁻⁵ of lithium vapor at the leading edge of the electron beam pulse $\sim 10 \mu\text{m}$ in diameter and $\sim 15 \mu\text{m}$ long. In the blow-out regime,⁶ the beam density is larger than the plasma density, and the electric field of the beam expels the cold electrons, which all end up at approximately the same radius. These electrons are drawn back in by the ions they left behind, and their oscillation forms a plasma wave on which electrons in the tail of the beam pulse surf to gain higher energy. The same mechanism does not work as well for positron acceleration, since the beam now *attracts* cold electrons from a spread in radius, and a coherent wakefield is not formed. A solution is to preform a hollow plasma by ionizing lithium vapor with an annular laser beam. The positron beam then attracts cold electrons starting from a well defined radius, thus improving the chances of creating a coherent wake.

The time delay between the laser pulse and the positron pulse is determined by the diffusion of the annular plasma. In classical diffusion of a cylindrical plasma, the initial fine structure decays rapidly until the lowest Bessel function mode remains, and this then decays at an exponential rate.⁷ If one assumes a cylindrical shell with absorbing boundaries at r_1 and r_2 , a Bessel function solution can easily be found, and it would decay with a time constant of about 2 ms. The current problem differs in two major respects. First, the diffusion coefficient varies by an order of magnitude with density, and hence with radius. Second, there is no absorbing boundary in the hole, and plasma fills the hole rapidly because of the strong gradients there. Higher harmonics can be generated rather than damped.

II. EXPERIMENTAL PARAMETERS

Single-photon ionization of oven-heated lithium vapor has been used as a plasma target for successful wakefield acceleration of 28-GeV positron beams.^{8,9} The 193 nm argon fluoride laser was focused into a 1.4 m long lithium oven with neutral density $n_n=2 \times 10^{15} \text{ cm}^{-3}$. In this paper, we assume that the laser beam is of order $500 \mu\text{m}$ in radius, and a beam block creates a hole of order $200 \mu\text{m}$ in radius. The laser intensity is adjusted to give a maximum density n_0 of order $2 \times 10^{14} \text{ cm}^{-3}$. These parameters were chosen to match experiments that have been attempted, but both the density and the size can be varied from those in this initial survey.

Near the density peak, diffusion is dominated by ion-ion collisions. At low density, it is dominated by ion-neutral charge-exchange collisions. Ions starting near the peak diffuse slowly because of frequent collisions with one another. As they spread out, their density decreases so that the rate of expansion is slowed only by the less frequent ion-neutral collisions. The situation is analogous to the bursting of a helium balloon. Initially, the helium gas expands at a rate determined only by He-He collisions. When the helium is mixed with air, it diffuses via He-air collisions. In a plasma, once the ion diffusion rate is determined, electrons will create an ambipolar electric field to speed up the diffusion.

The ion-ion collision frequency is¹⁰

$$\nu_{\perp}^{ii} = 1.4 \times 10^{-7} A^{-1/2} T_i^{-3/2} n \lambda_{ii} \text{ s}^{-1}, \quad (1)$$

where A is the atomic number, T_i the ion temperature in eV, n the plasma density in cm^{-3} , and λ_{ii} the appropriate Coulomb logarithm, given by

$$\lambda_{ii} = 22.7 - \ln(n^{1/2}/T_i^{3/2}). \quad (2)$$

This frequency falls linearly with n . The $\text{Li}^+\text{-Li}$ resonant charge exchange cross section σ_{cx} was given most conveniently by Lorentz *et al.*,¹¹ who fitted experimental points down to 14 eV with the formula

$$\sigma_{\text{cx}}(\text{Li}) = (a - b \log_{10} E_{\text{eV}})^2 \text{ cm}^2, \quad (3)$$

where $a=19.3 \times 10^{-8}$ and $b=3.5 \times 10^{-8}$. This formula was extrapolated to the lower energies of this problem. The col-

^{a)}Electronic mail: ffchen@ee.ucla.edu.

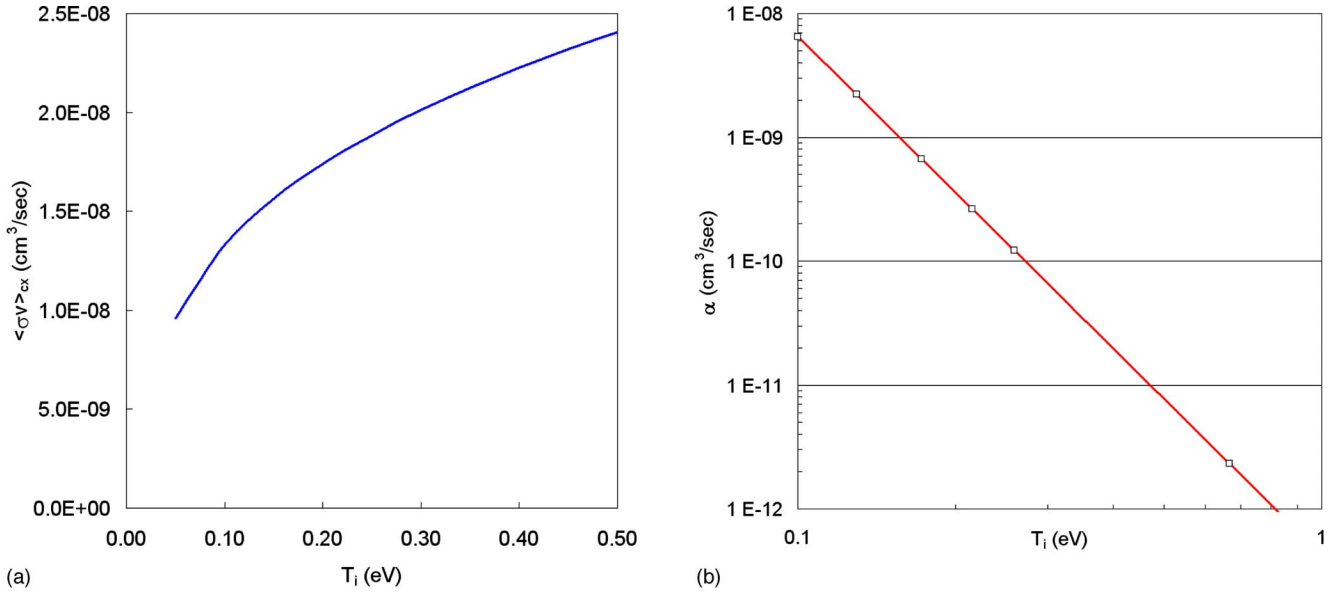


FIG. 1. (Color online) (a) Ion-neutral collision probability and (b) recombination coefficient vs lithium ion temperature.

lision probability $\langle\sigma v\rangle_{\text{cx}}$ was computed by integrating over a Maxwellian ion distribution at T_i and is shown in Fig. 1(a).

The ions are heated by electrons and cooled by the neutrals. Since the photon energy of the 193 nm laser is 6.45 eV and the lithium ionization energy is 5.39 eV, electrons are created with approximately 1 eV of average energy, corresponding to $(3/2)T_e$. Thus, $T_e \approx 0.67$ eV. The neutral gas has the oven temperature of 750 °C (≈ 1000 K), so that the ions start with the temperature $T_0 \approx 0.088$ eV. The equilibration time between ions and electrons is¹⁰

$$t_{\text{eq}} = 3.25 \times 10^8 A T_e^{3/2} / n \lambda_{ei}. \quad (4)$$

For $T_e = 0.67$ eV and $n \approx 2 \times 10^{14}$ cm⁻³, this gives $t_{\text{eq}} = 2.4$ μ s, which is much longer than the 50 ns timescales we shall find. Hence, T_i remains at ≈ 0.09 eV, at which $\langle\sigma v\rangle_{\text{cx}} \approx 1.3 \times 10^{-8}$ cm³/s. Thus, the ion-neutral collision frequency is

$$\nu_{io} = 1.3 \times 10^{-8} n_n \text{ s}^{-1}. \quad (5)$$

The measured radiative recombination coefficient α for hydrogenlike atoms has been given by Curry¹² [Fig. 1(b)] for T_e up to 3000 K and densities up to 10^{15} cm⁻³. Extrapolating to 0.67 eV (7700 K) yields $\alpha \approx 2.3 \times 10^{-12}$ cm³/s at $n = 2 \times 10^{14}$ cm⁻³. This turns out to be at most a 1% effect, but it is trivial to include it.

III. COMPUTATIONS

Diffusion of a cylindrically symmetric plasma is given by

$$\frac{\partial n}{\partial t} = D_a(n) \left(\frac{\partial^2 n}{\partial r^2} + \frac{1}{r} \frac{\partial n}{\partial r} \right) - \alpha n^2, \quad (6)$$

where D_a is the ambipolar diffusion coefficient⁷

$$D_a = D_i(1 + T_e/T_i) \quad (7)$$

and

$$D_i = KT_i/M\nu_{\text{tot}}. \quad (8)$$

Here, D_a depends on n but not explicitly on r . The total collision frequency ν_{tot} is the sum of the ion-ion part [Eq. (1)] and the ion-neutral part [Eq. (5)]. For $A=3$, $T_e = 0.67$ eV, and $T_i = 0.09$ eV, we have

$$\nu_{\text{tot}} = 1.3 \times 10^{-8} n_n + 8.3 \times 10^{-6} n \text{ s}^{-1}. \quad (9)$$

At 10% ionization, the ion-ion term is larger by a factor 64. This causes D_a to increase from 140 to 1300 cm²/s as n drops from 2×10^{14} cm⁻³ at the peak to 2×10^{13} cm⁻³ in the

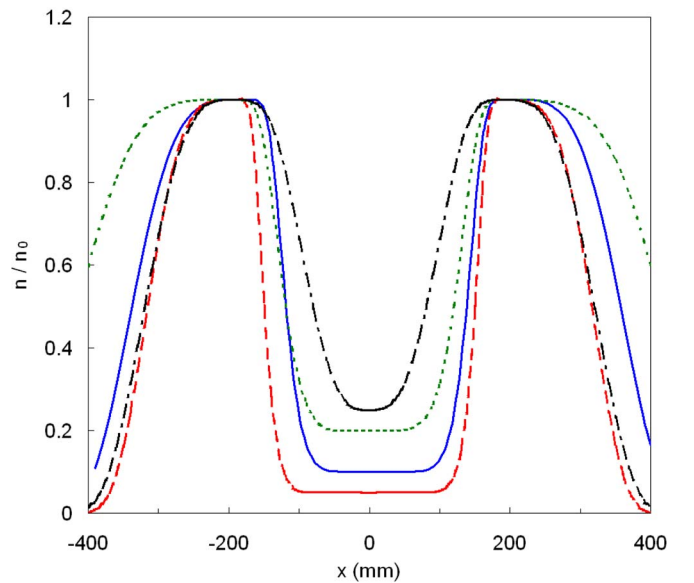


FIG. 2. (Color online) Hollow density profiles obtainable by varying the parameters f , s , t , u , v , and w for $r_0 = 200$ μ m.

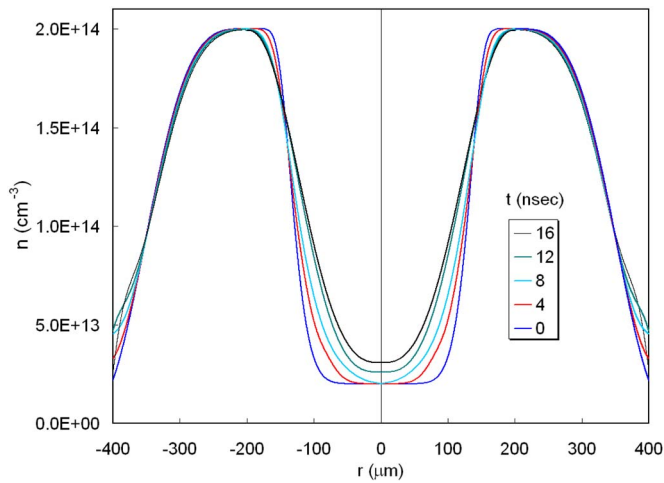


FIG. 3. (Color online) Decay of an annular plasma with a deep, wide hole. The order of the curves is obvious.

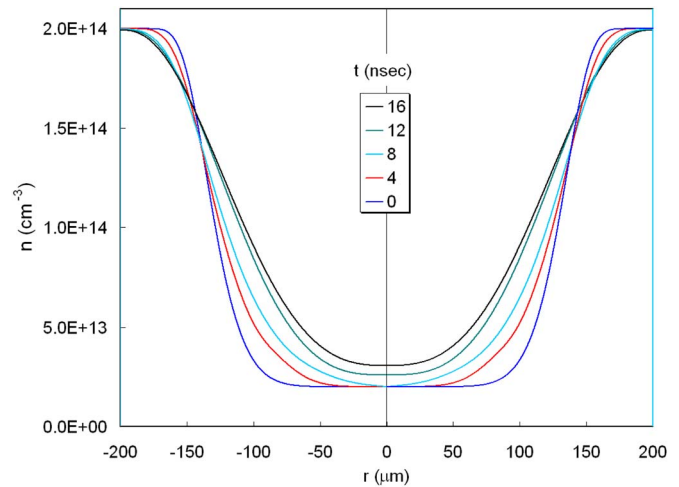


FIG. 5. (Color online) Detail of the inner region of Fig. 3.

hole and outside edge. Diffusion is an order of magnitude faster in the hole and foot of the density distribution.

The density initial density profile can be modeled with two three-parameter functions, one for $r \leq r_0$, and one for $r \geq r_0$, where r_0 is the radius of the beam block:

$$\frac{n}{n_0} = 1 + (f-1) \left[1 - \left(\frac{r}{r_0} \right)^s \right]^t, \quad r \leq r_0, \quad (10)$$

$$\frac{n}{n_0} = \left[1 - \left(\frac{r-r_0}{w} \right)^u \right]^v, \quad r \geq r_0. \quad (11)$$

Here, f is the fractional density at the center of the hole, and w is the half-width of the laser beam. These functions are chosen to join smoothly at $r=r_0$. The k th derivative of Eq. (10) vanishes for $k \leq t$, and the k th derivative of Eq. (11)

vanishes for $k \leq u$. Figure 2 illustrates density profiles obtainable by adjusting the six free parameters.

Equation (6) is solved by numerical differentiation using Stirling's rule. However, the procedure is not completely straightforward. Where the density is low, at the bottom of the trough and on the outside, the diffusion is extremely fast, and time steps have to be small in order to avoid unphysical peaks and oscillations in the density there. On the other hand, repeated double differentiations generate noise which cannot be smoothed without losing the shape of the curve. Thus, only two or three small time steps can be computed at a time. This problem was solved by fitting the last smooth curve to the analytic formulas of Eqs. (10) and (11) with different values of the parameters. When the nonlinearity introduced by $D(n)$ became too large, the fitting was done with a commercial curve-fitting program¹³ which uses, for instance, 20th-order Tchebyshev polynomials. The procedure is repeated many times.

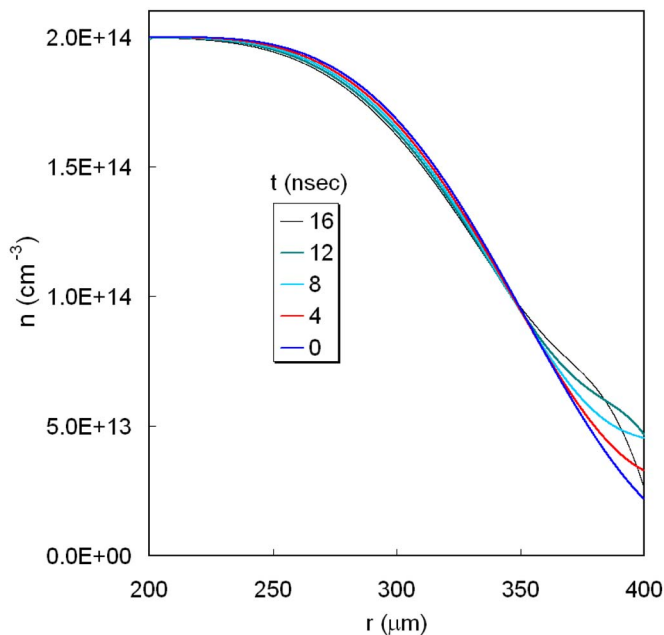


FIG. 4. (Color online) Detail of the outside part of Fig. 3.

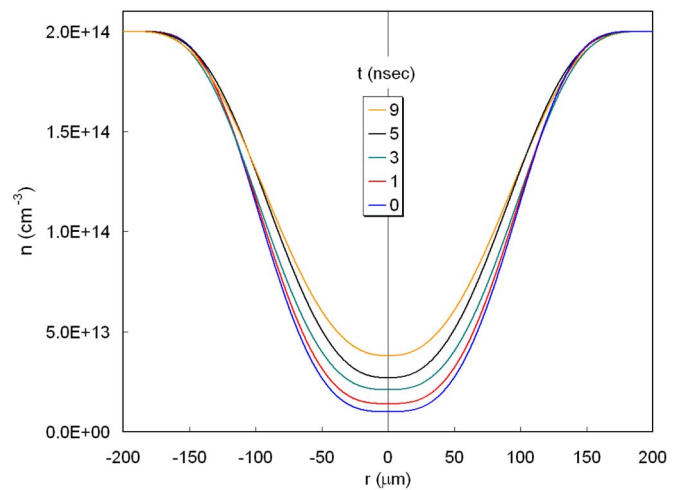


FIG. 6. (Color online) Diffusion of a profile with $r_0=200 \mu\text{m}$, $f=0.05$, $s=3$, $t=6$, and $n_0=2 \times 10^{14} \text{cm}^{-3}$.

IV. RESULTS

Figure 3 shows the evolution of a hollow profile characterized by $r_0=200\ \mu\text{m}$, $f=0.1$, $s=8$, $t=20$, $u=3.5$, $v=8$, $w=300$, and $n_0=2\times 10^{14}\ \text{cm}^{-3}$ in Eqs. (10) and (11). This profile has a large hole at a very low density, only 10% of the maximum. The center density fills in slowly because of the small gradients near the axis, changing noticeably only after about 10 ns. Figure 4 shows the outer region in more detail. The profiles can overlap at late times because the curvature can change nonmonotonically in nonlinear diffusion. In any case, the outside region is not of interest, and we focus on the density in the hole. Figures 5 and 6 compare the diffusion of two initial profiles differing in the slope of the density inside the hole. When the hole is not as sharply defined (Fig. 6) the larger gradients cause faster diffusion, and the center density changes noticeably after only about 2 ns. We conclude that there is a 1–10 ns window in which the positron bunches can be fired to generate wakefields, depending on the sharpness of the edge of the density hole.

At the maximum density of $2\times 10^{14}\ \text{cm}^{-3}$ treated here, the recombination term is 100 times smaller than the diffusion term. Since recombination varies as n^2 , it will be dominant above $n\approx 10^{16}\ \text{cm}^{-3}$, which useful positron acceleration requires. In that regime, the unusual diffusion mechanism found here would not be seen. We are indebted to Chan Joshi

for suggesting this problem, which turned out to be both interesting and nontrivial.

- ¹I. Blumenfeld, C. E. Clayton, F.-J. Decker, M. J. Hogan, C. Huang, R. Ischebeck, R. Iverson, C. Joshi, T. Katsouleas, N. Kirby, W. Lu, K. A. Marsh, W. B. Mori, P. Muggli, E. Oz, R. H. Siemann, D. Walz, and M. M. Zhou, *Nature (London)* **445**, 741 (2007).
- ²P. Chen, *Phys. Rev. Lett.* **54**, 693 (1985).
- ³W. P. Leemans, C. E. Clayton, W. B. Mori, K. A. Marsh, A. Dyson, and C. Joshi, *Phys. Rev. Lett.* **68**, 321 (1992); *Phys. Rev. A* **46**, 1091 (1992).
- ⁴D. L. Bruhwiler, *Phys. Plasmas* **10**, 2022 (2003).
- ⁵C. L. O'Connell, C. D. Barnes, F.-J. Decker, M. J. Hogan, R. Iverson, P. Krejcik, R. Siemann, D. R. Walz, C. E. Clayton, C. Huang, D. K. Johnson, C. Joshi, W. Lu, K. A. Marsh, W. Mori, M. Zhou, S. Deng, T. Katsouleas, P. Muggli, and E. Oz, *Phys. Rev. ST Accel. Beams* **9**, 101301 (2006).
- ⁶W. Lu, C. Huang, M. Zhou, W. B. Mori, and T. Katsouleas, *Phys. Rev. Lett.* **96**, 165002 (2006).
- ⁷F. F. Chen, *Intro. to Plasma Physics and Controlled Fusion*, 2nd ed. (Plenum, New York, 1984), Vol. 1, Sec. 5.2.3.
- ⁸M. J. Hogan, C. E. Clayton, C. Huang, P. Muggli, S. Wang, B. E. Blue, D. Walz, K. A. Marsh, C. L. O'Connell, S. Lee, R. Iverson, F.-J. Decker, P. Raimondi, W. B. Mori, T. C. Katsouleas, C. Joshi, and R. H. Siemann, *Phys. Rev. Lett.* **90**, 205002 (2003).
- ⁹B. E. Blue, C. E. Clayton, C. L. O'Connell, F.-J. Decker, M. J. Hogan, C. Huang, R. Iverson, C. Joshi, T. C. Katsouleas, W. Lu, K. A. Marsh, W. B. Mori, P. Muggli, R. Siemann, and D. Walz, *Phys. Rev. Lett.* **90**, 214801 (2003).
- ¹⁰D. L. Book, *NRL Plasma Formulary*, Naval Research Laboratory Publication 0084-4040, 1987.
- ¹¹D. C. Lorenz, G. Black, and O. Heinz, *Phys. Rev.* **137**, A1049 (1965).
- ¹²B. P. Curry, *Phys. Rev. A* **1**, 166 (1970).
- ¹³TableCurve 2D, SYSTAT Software, Inc.